r_i = dimensionless radius of annular ring (i), R/d_p
S = spreading factor
v = flow rate per unit of column area at any radial position, cm³/min
$\bar{v}$ = average flow rate per unit area over entire column, cm³/min
W = wall flow rate; W_j = wall flow rate at bed depth j; W_∞ = wall flow rate at equilibrium, cm³/min
z = bed depth, cm
δ = surface tension, dynes/cm

Subscripts

j = dimensionless bed depth, z/d_p; identification of particle in axial direction
∞ = equilibrium
i = annular ring (i) at any bed depth
m = annular ring next to the wall

LITERATURE CITED

Acres, G. J. K., "Trickle Column Reactors. Technique for the Continuous Performance of Liquid-Phase Catalyzed Reactions," *Platinum Metals Rev.*, **11**, 86 (1967).

Baker, T., T. H. Chilton, and H. C. Vernon, "The Course of Liquid Flow in Packed Towers," *Trans. Am. Inst. Chem. Engrs.*, 31, 296 (1935).

Charpentier, J. C., "Recent Progress in Two-Phase Gas-Liquid Mass Transfer in Packed Beds," *Chem. Eng. J.*, **11**, 161 (1976).

Jameson, G. J., "A Model for Liquid Distribution in Packed Columns and Trickle-Bed Reactors," *Trans. Inst. Chem. Engrs.*, 44, T198 (1966).

Levec, J., and J. M. Smith, "Oxidation of Acetic Acid Solutions in a Trickle Bed Reactor," *AIChE J.*, **22**, 159 (1976).

Onda, K., H. Takeuchi, Y. Maeda, N. Takeuchi, "Liquid Distribution in Packed Columns," *Chem. Eng. Sci.*, **28**, 1677 (1973).

Porter, K. E., J. J. Templeman, and V. D. Barnett, "II. The Spread of Liquid over Random Packings," *Trans. Inst. Chem. Engrs.*, **46**, T74 (1968).

Porter, K. E., and J. J. Templeman, "III. Wall Flow," *ibid.*, **46**, T86 (1968).

Prchlik, J., J. Soukup, V. Zapletal, and V. Ruzicka, "Liquid Distribution in Reactors with Randomly Packed Porous Beds," *Colln. Czech. Chem. Commun. (English)*, **40**, 845 (1975*a*).

———, "Wall Flow in Trickle Bed Reactor," *ibid.*, 3145 (1975*b*).

Ross, L. D., "Performance of Trickle-Bed Reactors," *Chem. Eng. Progr.*, **61**, 77 (1965).

Satterfield, C. N., and F. Ozel, "Direct Solid-Catalyzed Reaction of a Vapor in an Apparently Completely Wetted Trickle Bed Reactor," *AIChE J.*, **19**, 1259 (1973).

Satterfield, C. N., "Trickle-Bed Reactors," *ibid.*, **21**, 209 (1975).

Selby, S. M., ed., *Standard Mathematical Tables*, 19 ed., The Chemical Rubber Co., Sandusky, Ohio (1971).

Sheridan, M. B., and M. B. Donald, "The Mechanism of Liquid Flow in Packed Columns," *Ind. Chem.*, **35**, 439 (1959*a*).

———, "The Mechanism of Liquid Flow in Packed Columns," *ibid.*, 487 (1959*b*).

Soukup, J., K. Kolomaznik, V. Ruzicka, and J. Prchlik, "Spreading Coefficient in Randomly Packed Porous Beds," *Colln. Czech. Chem. Commun. (English)*, 38, 3742 (1973).

Specchia, V., A. Rossini, and G. Baldi, "Distribution and Radial Spread of Liquid in Two-Phase Concurrent Flows in a Packed Bed," *Ing. Chim. Ital.*, **10**, 171 (1974).

Manuscript received June 17, 1977; revision received December 5, and accepted December 16, 1977.

Part II. Tracer Studies

An aqueous solution of potassium chloride tracer was introduced at a central location in the water feed to a trickle bed, and the tracer concentration was measured at various radial positions and bed depths. From the model and parameters of liquid distribution proposed in Part I, tracer concentrations can also be predicted. The predicted and experimental concentrations usually agreed within a few percent, providing an independent evaluation of the flow distribution model.

SCOPE

Liquid distribution in packed beds can be evaluated indirectly from measurements of the radial spreading of a soluble tracer. Onda et al. (1973), Specchia et al. (1974), and Stanek and Kolar (1974) have made such measurements, particularly for the kinds of large particles used in absorption columns. The radial distribution was obtained by analyzing the data with a diffusion type of equation.

The theory for liquid distribution presented in Part I can be adapted to predict tracer concentrations as a function of radial position, packed-bed depth, and feed condition. Accordingly, we have measured tracer concentrations for conditions (particle size, liquid and gas flow rates) applicable to trickle-bed reactors. These data were then compared with predicted results in order to have an independent evaluation of the theory presented in Part I.

CONCLUSIONS AND SIGNIFICANCE

The flow distribution concepts proposed in Part I can be used to predict tracer concentrations by supposing that the streams entering a contact point, between adjacent annular rings, are completely mixed and leave with a uniform concentration. Such predictions differed from measured concentrations by no more than a few percent, except for some instances for the collector at the wall. The measurements were made for granular, spherical, and cylindrical particles in both the 4.08 and 11.4 cm I.D. columns. In view of the independence of distribution on liquid flow rate found in Part I, data were obtained for

each column at a constant flow rate. Measurements at gas flow rates covering a twentyfold range showed no discernible effect on tracer concentration, confirming the observations in Part I.

Variations in tracer concentration with operating procedure, repacking the bed, and fluctuations in liquid above the collector were much less than the variations in flow rate observed in Part I. Reproducibility of tracer data was about 5% in comparison with the 10% noted in the flow measurements.

Tracer data can be used instead of flow distribution data for evaluating the model parameters S and f. At conditions (particle size and shape, tube diameter, bed depth) for which flow reproducibility is a major problem, tracer measurements would be advantageous. For other conditions, the greater sensitivity of the flow data should give more accurate values of the model parameters. Also, the tracer method cannot be used, with experimental data obtained from concentric collectors, to evaluate directly the wall flow rate.

EXPERIMENTAL

The columns, collectors, and uniform feed distribution equipment described in Part I were used for the tracer experiments. An aqueous potassium chloride solution (1.0 molal) was fed to the top of a centrally located tube (0.540 cm I.D. for the 11.4 cm column and 0.238 cm I.D. for the 4.08 cm column,) while the gas entered in concurrent flow through an annulus around this central tube. Dimensions and locations of the tubes for providing a uniform flow of water and for injecting the gas are the same as described in Part I. The tube containing the aqueous potassium chloride solution terminated 0.5 cm above the top of the particles in the 11.4 cm column and 0.3 cm above for the 4.08 cm column.

Water and tracer solution flow rates were adjusted so that the velocities in the feed tubes were of the same magnitude for both streams. Operating conditions are summarized in Table 1.

Tracer concentrations in samples from each section of the collector were determined with a conductivity cell and bridge apparatus (model RC-1B, manufactured by Industrial Instruments, Inc.). The Rostock equation (Janz and Tomkins, 1977) was used to relate the observed conductivity to the concentration. Measurements over the range 0.001 to 1.0 molal with standard samples indicated a maximum deviation of less than 1%, provided the temperature of the cell was maintained reasonably constant. For this purpose, we used a thermostatic water bath operated at 25 ± 0.1°C.

The method of packing the column and the operating procedure was the same as described in Part I. Steady state was reached within 3 min following the initiation of tracer flow. Three samples were collected in each section over an interval of 20 min. The variation in tracer concentration between samples was less than 5% for all conditions. Data were taken for several particles over a range of packed-bed depth as shown in Table 2.

PREDICTED TRACER DISTRIBUTION

In Part I, the distribution of liquid was predicted by dividing the packed bed radially and axially into annular rings of width and height equal to the particle diameter.

Table 1. Operating Conditions for Tracer Experiments

Column, I.D., cm	4.08	11.4
Tracer solution flow rate,* cm³/s	0.18	0.18 to 0.33
Liquid superficial velocity, cm/s	0.39**	0.12**
Gas superficial velocity, cm/s	1.0	0.1 to 2.0
Collector†	A (three sections)	B (four sections)

† Description of collectors A and B are given in Part I, Table 1.
* 1.0 molal aqueous potassium chloride solution.
** The water flow rate varied slightly from run to run, and individual values were used in obtaining the results presented in Table 2. All values corresponded approximately to the superficial velocities given here. The water rate includes the water in the tracer solution fed to the column.

Liquid flow is exchanged at contact points between adjacent rings (Figures 7 to 9, Part I). The same concepts are used here to predict tracer distribution with the additional assumptions that complete mixing of tracer occurs at the contact points and that the liquid leaving each annular ring is well mixed. As in Part I, the two streams that leave each contact point for adjacent annular rings are assumed to be of equal flow rates. The streams leaving ring (i, j) for the contact points and the flows leaving the contact points for rings $(i-1, j+1)$, $(i, j+1)$, and $(i+1, j+1)$ are shown in Figure 1. Other assumptions are that molecular diffusion of tracer is negligible and that the bed is uniformly packed (no radial variation in void fraction) except near the wall.

The liquid flow $F_{i,j}$ that leaves annular ring i,j divides into three streams, I, II, III as in Part I and as shown in Figure 1, each of which has a tracer concentration $C_{i,j}$. One stream with a molal flow rate of tracer of $\left(\frac{S}{2}\right)\frac{2r_i-1}{2r_i}F_{i,j}C_{i,j}$ goes to the mixing point between the (i, j) and $(i-1, j)$ rings; another of tracer flow rate $\left(\frac{S}{2}\right)\frac{2r_i+1}{2r_i}F_{i,j}C_{i,j}$ goes to the mixing point between rings (i, j) and $(i+1, j)$. The third stream of tracer flow rate $(1-S)F_{i,j}C_{i,j}$ goes directly to annular ring $(i, j+1)$. This bypassing stream is joined by the two streams IV and V from the mixing points to constitute the total flow to the $(i, j+1)$ ring. A mass balance of tracer for the annular ring $(i, j+1)$ requires that the flow of tracer into the ring via the three streams be equal to the tracer leaving the ring. This balance may be written as

$$F_{i,j+1}C_{i,j+1} = \left(1-\frac{S}{2}\right)F_{i,j}C_{i,j} + \frac{S}{4}\left[\left(\frac{2r_i-1}{2r_i-2}F_{i-1,j}C_{i-1,j} + \frac{2r_i+1}{2r_i+2}F_{i+1,j}C_{i+1,j}\right)\right] \quad (1)$$

Equation (1) is applicable for $i = 2$ to $m-1$ and $j = 1$ to n. At the center annular ring there are contact points only between annular rings $(1, j)$ and $(2, j)$. Hence, the mass balance for the center ring takes the form

$$F_{1,j+1}C_{1,j+1} = \left[1-\left(\frac{S}{8}\right)\frac{2r_1+1}{r_1}\right]F_{1,j}C_{1,j} + \frac{S}{8}\frac{2r_1+1}{r_1+1}F_{2,j}C_{2,j} \quad (2)$$

The flow network for the annular ring (m, j) at the wall is the same as shown in Figure 9 of Part I. The molar flow

TABLE 2. COMPARISON OF EXPERIMENTAL AND PREDICTED RESULTS

Particle	Equivalent particle diam., cm	Bed depth, cm	Tracer soln flow rate, cm³/s	S	f	$C_o \times 10^5$ moles/cm³	Experimental and predicted tracer concentrations							
							$C_{E,I}/C_o$	$C_{T,I}/C_o$	$C_{E,II}/C_o$	$C_{T,II}/C_o$	$C_{E,III}/C_o$	$C_{E,IV}/C_o$	$C_{T,IV}/C_o$
Activated carbon*	0.875	0	0.18	0.80	0.62	1.57	3.56		0		0	0	
		28	0.18			1.57	1.43	1.46	1.11	1.19	0.958	0.828	0.782
		28	0.33			2.86	1.45	1.47	1.14	1.19	0.958	0.819	0.782
Alumina cylinders*	0.778	0	0.18	0.80	0.53	1.60	3.65		0		0	0	
		21	0.18			1.60	1.65	1.57	1.01	1.05	0.625	0.644	0.369
		21	0.33			3.10	1.68	1.57	1.01	1.05	0.625	0.644	0.369
Ceramic cylinders*	0.898	0	0.18	0.70	0.48	1.64	3.88		0		0	0	
		30	0.18			1.64	1.35	1.42	1.07	1.14	0.835	0.823	0.737
		30	0.18			1.64	1.28	1.42	1.14	1.14	0.835	0.823	0.737
		40	0.18			1.64	1.15	1.23	1.03	1.06	0.964	0.878	0.811
		49	0.18			1.69	1.02	1.15	1.02	1.05	0.988	0.936	1.01
Ceramic balls*	0.635	0	0.18	0.90	1.00	1.40	4.16		0		0	0	
		20	0.18			1.40	1.79	1.95	1.21	1.08	0.542	0.564	0.443
		30	0.18			1.43	1.40	1.49	1.07	1.05	0.754	0.768	0.803
		41	0.18			1.62	1.13	1.23	0.998	1.01	0.850	0.875	0.998
		50.5	0.18			1.62	1.04	1.12	1.03	0.998	0.998	0.918	0.949
Activated carbon†	0.352	0	0.18	1.00	0.57	3.67	3.33		0		0	0	
		5.9	0.18			3.67	1.49	1.44	0.736	0.787	0.491	0.488	0.782
		10.2	0.18			3.67	1.22	1.13	0.909	0.895	0.752	0.713	0.888

* 11.4 cm column.
† 4.08 cm column.

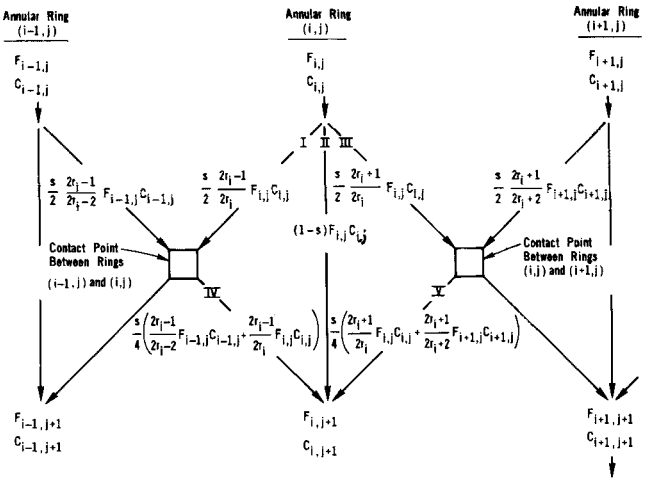

Fig. 1. Tracer concentration network in the bed.

rate of tracer to and from the mixing point between annular ring (m, j) and the wall is illustrated in Figure 2. Note that there is a tracer flow along the wall of $(1-f)W_j C_{m+1,j}$. The mass balances for tracer over annular ring (m, j) and at the wall are

$$F_{m,j+1}\,C_{m,j+1} = f^2 W_j\,C_{m+1,j} + \left(\frac{fS}{2}\,\frac{2r_m+1}{2r_m} + \frac{S}{4}\,\frac{2r_m-1}{2r_m} + 1 - S\right) F_{m,j}\,C_{m,j} + \frac{S}{4}\,\frac{2r_m-1}{2r_m-2}\,F_{m-1,j}\,C_{m-1,j} \quad (3)$$

$$W_{j+1}\,C_{m+1,j+1} = (1-f)\left[(1+f)W_j\,C_{m+1,j} + \frac{S}{2}\,\frac{2r_m+1}{2r_m}\,F_{m,j}\,C_{m,j}\right] \quad (4)$$

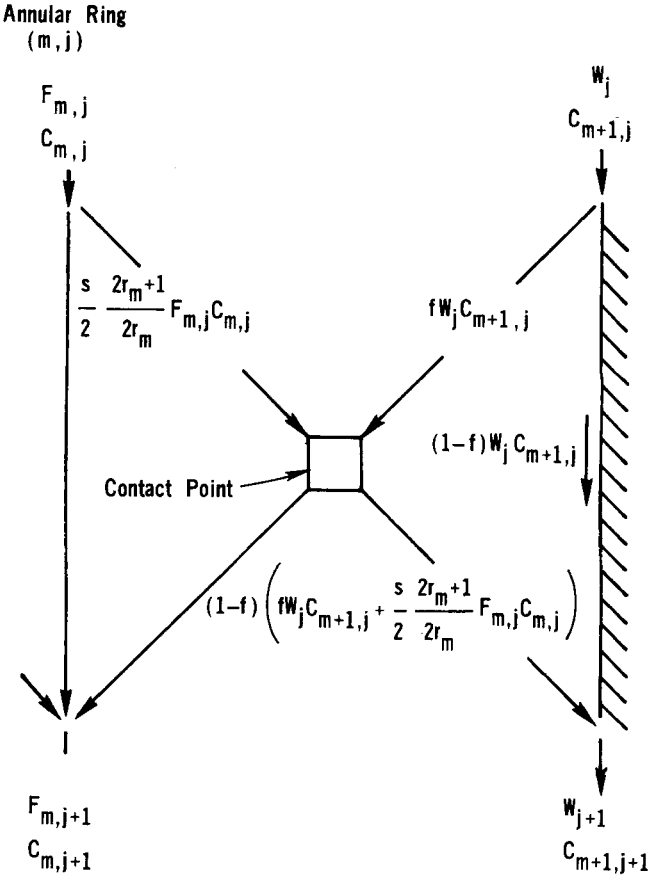

Fig. 2. Tracer concentration network at the wall.

Equations (1) to (4) are analogous to Equations (2) to (5) of Part I, and the two sets of equations may be used to predict the tracer concentration at any radial and axial position from a known tracer distribution at the feed point $j = 1$. The procedure is initiated by calculating the tracer concentration for annular rings at $j = 2$, $i = 1$ to m, from the equations. Then this step is repeated until the required bed depth ($j = n$) is reached. The computations require only the values of the spreading factor S and the wall factor f which are correlated in Figures 10 and 11 of Part I for the air-water system.

COMPARISON OF PREDICTED AND EXPERIMENTAL RESULTS

The experimental results are given in Table 2 in the columns headed $C_{E,k}/C_o$. These values are the ratios of the measured concentration in section k of the collector to the average concentration of tracer introduced in the feed. The la ter quantity is equal to the molal flow rate of tracer introduced in the central tube of the distributor divided by the total feed rate of water. The results listed in Table 2 for the first two kinds of particles show that there was not a significant effect on $C_{E,k}/C_o$ when the tracer solution flow rate was increased from 0.18 to 0.33 cm³/s. The reproducibility of the data is illustrated by the two sets of measurements shown for the 0.898 cm ceramic cylinders at a bed depth of 30 cm and with a tracer solution flow rate of 0.18 cm³/s. The two sets of data were obtained by repacking the bed. Of the five particle-column combinations tested, the flow distribution at equilibrium was nonuniform ($W \neq 0$) except for the 0.635 cm ceramic balls.

The average deviation for all the measurements was less than 5% in comparison with 10% deviation for flow rate data. Apparently, the concentrations determined in each section of the collector, representing average values, are not as sensitive to minor fluctuations in flow rate. A mass balance of tracer was made on each run to test reliability. The molal rate of tracer obtained by summing the products of the flow rate and concentration in each section of the collector was always within 5% of the tracer feed rate.

The predicted concentrations of tracer in each section of the collector were calculated by adding the tracer flow in all the annular rings in the section. For example, for section k

$$C_{T,k} = \frac{(\sum_i F_{i,n}C_{i,n}) + W_n C_{m+1,n}}{(\sum_i F_{i,n}) + W_n} \qquad (5)$$

where the summations apply to the annular rings in section k and the subscript n designates the desired bed depth, that is, $L = nd_p$. The terms involving W_n in Equation (5) are zero for all sections except the section at the wall. The concentrations $C_{i,n}$ and $C_{m+1,n}$ in the annular rings and in the wall flow were evaluated from Equations (1) to (4). The corresponding flow rates $F_{i,n}$ and W_n were calculated with Equations (2) to (5) of Part I. These calculations were carried out by starting at the top of the bed ($j = 1$) where the tracer and flow distributions are known. Thus, all the tracer is in annular ring $i = 1$, $j = 1$, and the flow is uniform. These values are used in Equations (1) to (4) to calculate concentrations at $j = 2$. This process is repeated until the desired bed depth $j = n$ is reached. Finally, the concentrations $C_{T,k}$ are determined from Equation (5). The necessary values of S and f were obtained for each particle-column combination from Table 4 of Part I. The predicted concentrations and parameter values are also given in Table 2. For all sections within the bed, agreement between experimental and predicted concentrations is within a few percent. Deviations are larger in the section nearest the wall (maximum deviation is 17%). Computations with varying values of S and f indicate that $C_{T,k}$ at the wall is sensitive to S and f. This is because small errors in these parameters affect both $C_{m+1,j}$ and W_j, and these quantities are required in Equation (5) in order to obtain $C_{T,k}$ for the wall section. Furthermore, it was observed in Part I that wall flow rates were the most difficult to reproduce. These reasons probably explain the larger deviations in the section nearest the wall.

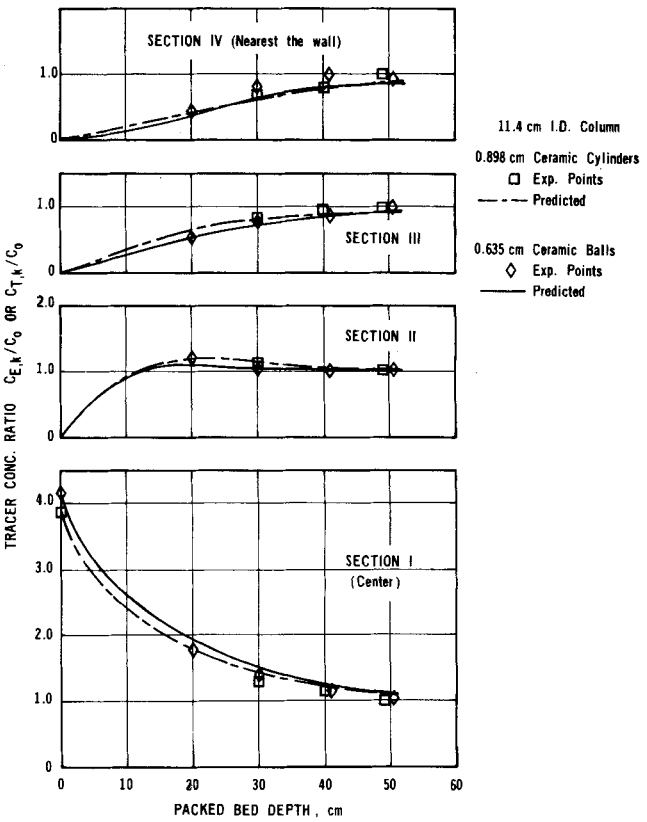

Fig. 3. Tracer concentration profiles.

At bed depths for which equilibrium is approached, the tracer concentration should be nearly uniform in the radial direction. Such a uniform concentration, equal to C_o, would be attained regardless of whether there is a nonuniform flow distribution. The model provides for this by the exchange of liquid between the wall and the bed (Figure 2). Both experimental and predicted concentrations show such results. This is illustrated in Figure 3, where experimental and predicted concentration ratios are plotted vs. bed depth for two types of particles.

Tracer measurements such as those reported here could be used to evaluate the model parameters S and f by the reverse of the procedure described for predicting concentrations from known values of S and f. However, the wall flow W_j could not be obtained directly from the tracer data. It would have to be calculated from Equation (5) of Part I using the model parameters. This is in contrast to the flow distribution measurements, where W_j is obtained from the experimentally determined flow rates in the collectors.

ACKNOWLEDGMENT

The financial assistance of the National Science Foundation, Grant ENG76-00153, is gratefully acknowledged. We also thank R. W. Powell for his assistance in the experimental work.

NOTATION

C_o = average concentration of the tracer, defined as the molal flow rate of tracer divided by total flow rate of water, moles/cm^3

$C_{i,j}$ = tracer concentration in annular ring (i, j), moles/cm^3

$C_{i,n}$ = tracer concentration in annular ring i at bed depth n $(=L/d_p)$, moles/cm^3

$C_{m+1,j}$ = concentration of tracer in the wall flow, moles/cm^3

$C_{E,k}$ = experimental tracer concentration in section k of collector, moles/cm^3

$C_{T,k}$ = predicted tracer concentration in section k of collector, moles/cm^3

k = identification of section in collector, that is, k = I, II, III

LITERATURE CITED

Janz, G. J., and R. P. T. Tomkins, "Conductance Cell Calibrations: Current Practices," *J. Electrochem. Soc.*, **124**, 55C (1977).

Onda, K., H. Takeuchi, Y. Maeda, and N. Takeuchi, "Liquid Distribution in Packed Columns," *Chem. Eng. Sci.*, **28**, 1677 (1973).

Specchia, V., A. Rossini, and G. Baldi, "Distribution and Radial Spread of Liquid in Two-Phase Concurrent Flows in a Packed Bed," *Ing. Chim. Ital.*, **10**, 171 (1976).

Stanék, V., and V. Kolár, "The Radial Spread and the Number of Rivulets in a Trickle Bed," *Colln. Czech. Chem. Commun.*, 39, 2007 (1974).

Manuscript received June 17, 1977; revision received December 5, and accepted December 16, 1977.

The Design of Gas Sparged Devices for Viscous Liquid Systems

S. M. BHAVARAJU

T. W. F. RUSSELL

and

H. W. BLANCH

Department of Chemical Engineering
University of Delaware
Newark, Delaware 19711

Design procedures for gas sparged contactors for both low and high viscosity liquids were developed to predict overall k_La. Bubble size close to the orifice, for moderately high gas rates, was found to increase at a rate proportional to one third power of gas rate and one tenth power of liquid viscosity. Bubble breakup phenomenon was shown to be related to liquid turbulence in the vessel rather than gas turbulence in the orifice. Procedures were developed through a simple liquid circulation model to obtain a criterion for the onset of bubble breakup. Results indicate that intense liquid mixing and high interfacial area can be achieved in low viscosity liquids by gas sparging alone. In high viscosity fluids, bubble breakup was not observed. The liquid circulation model predicts laminar flow at these experimental conditions over the complete range of gas rates observed.

SCOPE

Simple and useful procedures for designing gas-liquid contactors for a highly viscous liquid phase are not available. Some procedures exist for low viscosity liquids, but previous investigations of gas sparging in high viscosity liquids were restricted to the study of bubble formation at low gas rates near the orifice. No studies have been reported on bubble breakup phenomena at commercial scale gas rates, in either high or low viscosity systems. The hypothesis reported in the literature, that gas turbulence in the orifice can be correlated with bubble breakup and increased interfacial area, was found to fail when liquid viscosity was increased. A design procedure to predict bubble diameters as a function of gas rate, orifice diameter, and liquid viscosity for moderately high gas rates needs to be developed which is simple enough for practical use. A mechanistic model to study the bubble breakup phenomena in the commercial scale gas rate range for both low and high viscosity liquids also needs to be formulated (based on liquid turbulence rather than gas turbulence).

CONCLUSIONS AND SIGNIFICANCE

It is important in the design and scale-up of gas-liquid contactors to be able to predict mass transfer coefficients and interfacial area per unit volume independently. Design procedures for gas-liquid contactors for both low and high viscosity liquids were developed to obtain liquid phase mass transfer coefficient k_L and interfacial area a to predict the overall k_La. Results of the liquid circulation model indicate that bubble breakup, leading to higher interfacial area, depends on the liquid turbulence in the vessel rather than gas turbulence in the orifice.

Design procedures to predict both the mass transfer coefficient k_L and the interfacial area in gas sparged tanks are presented. The procedures are valid for a wide range of liquid viscosities and gas flow rates and show for the first time the prime importance of liquid circulation and turbulence. Inclusion of liquid circulation in the model allow one to be more confident in the commercial scale design.

The design procedures show that intense liquid mixing

0001-1541-78-1142-0454-$01.55.